Greatly enhanced risk to humans as a consequence of empirically determined lower moist heat stress tolerance

Daniel J. Vecellio[a,1,2] (iD), Qinqin Kong[b,1] (iD), W. Larry Kenney[a,c,d] (iD), and Matthew Huber[b] (iD)

As heatwaves become more frequent, intense, and longer-lasting due to climate change, the question of breaching thermal limits becomes pressing. A wet-bulb temperature (T_w) of 35 °C has been proposed as a theoretical upper limit on human abilities to biologically thermoregulate. But, recent—empirical—research using human subjects found a significantly lower maximum T_w at which thermoregulation is possible even with minimal metabolic activity. Projecting future exposure to this empirical critical environmental limit has not been done. Here, using this more accurate threshold and the latest coupled climate model results, we quantify exposure to dangerous, potentially lethal heat for future climates at various global warming levels. We find that humanity is more vulnerable to moist heat stress than previously proposed because of these lower thermal limits. Still, limiting warming to under 2 °C nearly eliminates exposure and risk of widespread uncompensable moist heatwaves as a sharp rise in exposure occurs at 3 °C of warming. Parts of the Middle East and the Indus River Valley experience brief exceedances with only 1.5 °C warming. More widespread, but brief, dangerous heat stress occurs in a +2 °C climate, including in eastern China and sub-Saharan Africa, while the US Midwest emerges as a moist heat stress hotspot in a +3 °C climate. In the future, moist heat extremes will lie outside the bounds of past human experience and beyond current heat mitigation strategies for billions of people. While some physiological adaptation from the thresholds described here is possible, additional behavioral, cultural, and technical adaptation will be required to maintain healthy lifestyles.

wet-bulb temperature | heat stress | extreme heat | human adaptability | climate change

Global mean surface air temperatures have risen by about 1 °C in the past century and are projected to increase by another 1–6 °C by 2100 depending on future greenhouse gas emissions and the model used (1). As a result of the increase in mean temperatures, heatwaves—as measured by dry-bulb temperature—have become more severe, frequent, and prevalent (2–4). These changes are expected to continue into the future (5, 6). While model predictions are always accompanied by uncertainties, it is important to note that climate models consistently underpredict the probability of extreme events (7), so the expected impact of climate change on future heatwaves may be biased too low. These expected (and perhaps, unexpected) future extreme heat events put the viability of some geographic regions being conducive for healthy and comfortable living into question (8).

The epidemiological and physical foundations for this concern for public health and welfare are clear. Heat is the leading type of weather fatality in the United States (9) and one of the largest causes of weather-related deaths worldwide. It increases the risk of both morbidity and mortality in vulnerable groups such as the elderly, children, outdoor workers, and those with comorbidities or those taking medication that causes diminished thermoregulatory capabilities (10, 11). Heatwaves are associated with increased hospitalization and death for cardiovascular, respiratory, and renal ailments as well as diabetes (12–14). These specific outcomes are not solely due to the body becoming too hot, but rather are compounded by the physiological strain extreme heat puts on the body and the body having to compensate to cool itself. Direct heat-related death (i.e., heat stroke) occurs when the core (internal) temperature of the body becomes too high due to the fact that it no longer has the capability to cool itself and biological functions cease (15).

Prior thresholds underlain by physiological theory set the upper limit of the human body's adaptability to extreme heat at a wet-bulb temperature (T_w) of 35 °C (16), also popularly referred to as the human adaptability or survivability limit. T_w is a measure of the moist enthalpy in the atmosphere and is thus thermodynamically equivalent to other proposed moist heat stress measures (17, 18) but has a longer history and simpler physiological interpretation. Dating back to Haldane's pioneering work (19), T_w has

Significance

Increased heat and humidity potentially threaten people and societies. Here, we incorporate our laboratory-measured, physiologically based wet-bulb temperature thresholds across a range of air temperatures and relative humidities, to project future heat stress risk from bias-corrected climate model output. These vulnerability thresholds substantially increase the calculated risk of widespread potentially dangerous, uncompensable humid heat stress. Some of the most populated regions, typically lower-middle income countries in the moist tropics and subtropics, violate this threshold well before 3 °C of warming. Further global warming increases the extent of threshold crossing into drier regions, e.g., in North America and the Middle East. These differentiated patterns imply vastly different heat adaption strategies. Limiting warming to under 2 °C nearly eliminates this risk.

[1]D.J.V. and Q.K. contributed equally to this work.

[2]To whom correspondence may be addressed. Email: dvecelli@gmu.edu.

been a useful measure in the description of human heat stress (16, 20–24) as a sweat-covered human body acts much like the wet wick of a wet-bulb thermometer. Given that optimal human core temperature is 37 °C, an internal thermal gradient conducive to moving metabolic heat from the core to the periphery of the body via skin blood flow would stipulate that skin temperature must remain below a maximum temperature of 35 °C. When the ambient environment reaches T_w = 35 °C, the body would be no longer able to thermoregulate via conduction and convection of heat brought to the skin via blood flow or evaporation of sweat on the surface of the skin. Importantly, Sherwood and Huber (16) stated that this was an upper bound and proposed that a lower number would be more realistic, but an exact lower estimate was not estimated. They found that warming above this threshold did not become widespread and persistent until global warming was above 6 °C.

Recent empirical work in young, healthy subjects performing minimal metabolic workloads has supported a lower, varying T_w threshold, constant in warm, humid environments [30.6 °C up to T_a = 40 °C, 50% relative humidity (RH)], decreasing in a linear fashion from there with lower RH and higher air temperatures (21) (*Materials and Methods*). At these T_w thresholds, while subject core temperatures were still well below values relating to heat exhaustion or stroke, they did begin to rise continuously without impediment, defined as uncompensable heat stress. This condition is the basis of Sherwood and Huber's (16) theoretical physiological limit to heat adaptation. While core temperatures associated with this limit do not represent an immediate danger, prolonged exposure on the order of 6 h would lead to increased risk of heat-related illness or even death, even in young, healthy adults under conditions of minimal exertion(25).

Previous work has looked at historical observations as well as future climate projections to determine regions of the world that have exceeded the T_w = 35 °C upper limit of human adaptability or will be at risk to do so in the future. Observations have shown that on rare occasions, for an hour or two at a time, T_w > 35 °C

have been observed in the Middle East and South Asia (22). These regions are also expected to be main hotspots of future threshold exceedance (23). Other studies have used CMIP6 model output to estimate exceedance of thresholds associated with other heat stress indices such as the wet bulb globe temperature (WBGT), the Universal Thermal Climate Index (UTCI), and apparent temperature in addition to the previously described 35 °C T_w limit (26). However, given the collected empirical data establishing a lower criterion for heat stress compensability, it is important to update our understanding of regions of the world which have become too hot for normal activities or will in the future. Here, we examine future threshold exceedance based on updated empirical heat stress thresholds (*Materials and Methods*) using bias-corrected, down-scaled CMIP6 output to examine the spatiotemporal expansion of ambient environments inimical to human well-being in the future. Additionally, given the varying nature of the T_w threshold with increasing T_a/decreasing RH, we quantify the spatiotemporal pattern of heat stress types (humid vs. nonhumid), which plays a large role in how future adaptation will need to develop.

Global and Regional Variability in Emergence of Uncompensable Heat Stress

The magnitude and spatial extent of uncompensable heat stress increases as expected from theory (16, 17, 27, 28) with every degree of global mean surface temperature (GMST) warming or "global warming levels." Regional emergence of dangerous moist heat is heterogeneous in relation to future warming levels as semiequatorial regions first experience some hours of threshold exceedance at 1.5 °C warming above preindustrial levels (and likely before), while other parts of the globe remain safe until the GMST increase reaches 4 °C (Fig. 1 *A–D*). With increased global warming, the regions that will experience the first moist heat waves and subsequent substantial increases in accumulated hot-hours per year are also the regions with the largest concentrations
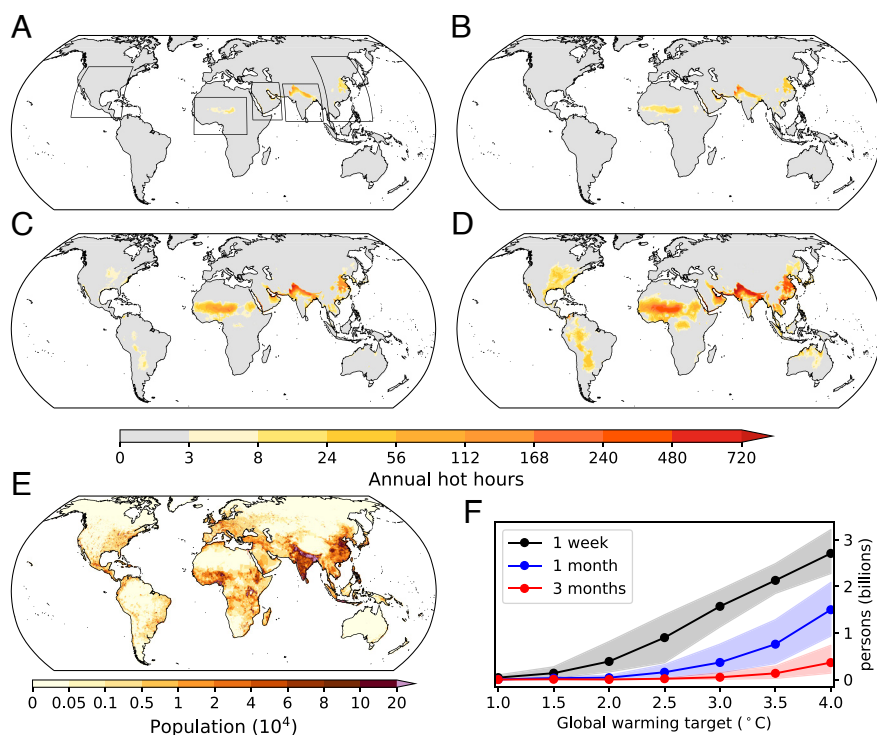

Fig. 1. Annual hot-hours under (*A*) 1.5, (*B*) 2, (*C*) 3, and (*D*) 4 °C of warming relative to preindustrial level, (*E*) population projection in 2050 following the Shared Socioeconomic Pathway 2, and (*F*) population subject to accumulated duration of 1 wk to 3 mo of uncompensable heat stress annually under 1–4 °C of global warming (the shaded area corresponds to the 10th to 90th percentiles of CMIP6 model spread). Rectangles in panel a delineate regions where heat exposure increases with global warming are particularly large and will be examined in detail in later sections.

Table 1. Global person-hours of threshold exposure (in millions) under different threshold scenarios across global warming levels

Warming level	$T_w = 35\ °C$ limit	Empirical limit
1.5 °C	9.24	43,955.60
2 °C	21.45	86,293.83
3 °C	818.78	349,839.33
4 °C	5,584.99	108,0327.89

of the world's population, specifically, those in India and the Indus River Valley (population: 2.2 billion), eastern China (population: 1.0 billion), and sub-Saharan Africa (population: 0.8 billion) (Fig. 1E). These also are generally home to lower-to-middle income countries and hence represent some of the world's most vulnerable populations.

Extended Data, *SI Appendix,* Fig. S1A shows the global extent of threshold exceedance at the previous theoretical upper limit of $T_w = 35\ °C$ at 4° GMST warming. A minimal amount of annual hot-hours are confined to sub-Saharan Africa and the Indus Valley at $T_w = 35\ °C$, comprising a small fraction of the spatial extent of substantial annual hot-hour accumulation when applying the empirical thresholds at 4 °C GMST warming (Fig. 1D). As a result, the number of person-hours of exposure to dangerous heat-health conditions using a $T_w = 35\ °C$ threshold is severely underestimated (Table 1).

In climate change scenarios of 2 °C warming and below, conditions associated with threshold exceedance are limited to the Indus River Valley, east China, the Persian Gulf coastline, and sub-Saharan Africa. Increases in the number of hours over the threshold in these regions are mild in transitioning from 1.5 °C to 2 °C (Fig. 1 A and B). Most of these regions are doubly exposed to extreme heat environments because of high incoming solar radiation causing high land temperatures in conjunction with proximity to water bodies with climatologically high sea surface temperatures. Monsoon dynamics are also likely to exacerbate such conditions, such as in South Asia and east China, and should continue to do so in the future with a projection of increased associated moisture in the seasonal events (29).

In future climates characterized by 3 °C and 4 °C GMST increases (Fig. 1 C and D), moist heat stress deepens, and these regions see significant increases in the number of annual hours above the heat stress thresholds. In addition, the affected area broadens, and regions of North and South America begin to exhibit an accumulation of hot-hours in the +3 °C warmer world (Fig. 1C), while northern and central Australia begin to experience an accumulation of hours above the threshold once GMSTs reach 4 °C above the preindustrial baseline (Fig. 1D).

These large-scale patterns are strongly modulated by regional and local scale climate processes and geography. To estimate risk to people requires further consideration of population distributions. Regionally, southwest Asia dominates the population-based distribution of hot-hours across the four warming scenarios presented (Fig. 2 A–D). While impacts are fairly contained to eastern Pakistan and the Indus River Valley in northern India in the 1.5 °C and 2 °C warming scenarios, they expand greatly in 3 °C and 4 °C warmer worlds with substantial accumulation of annual hot-hours along the Indian coast of the Bay of Bengal as well as into the countries of Bangladesh and parts of Myanmar. Heat stress also dominates the highly populated cities of East Asia (Fig. 2 E–H). As in southwest Asia, dangerous heat-health conditions stay clustered up until 4 °C, primarily in the highly populated cities of eastern China such as Shanghai, Nanjing, and

Wuhan. However, with future warming, the coastal regions of Japan, Korea, Cambodia, Laos, and Thailand also begin to experience increased accumulations of hot-hours with cities such as Tokyo, Seoul, Bangkok, and Ho Chi Minh City affected (Table 2). In Africa, the heat stress signal increases in magnitude and extent with every degree of GMST increase, spreading radially outward from the middle of the Sahel to the Atlantic Ocean and Gulf of Guinea coastlines as GMST increases (Fig. 2 I–L).

Coastal influences, be it ocean, sea, or river, are seen in the Middle East (Fig. 2 M–P) and North America (Fig. 2 Q–T). Cities along the west coast of Saudi Arabia (Jeddah and Mecca) and Yemen (Al Hudaydah) experience a substantial number of hours of threshold exceedance (Table 2), but the signal quickly diminishes off-shore. Land areas around the Persian Gulf experience heat stress with penetration deeper into the interior occurring in the United Arab Emirates, namely Dubai, and southeastern Saudi Arabia. In North America, heat stress signals begin to appear at 3 °C GMST warming but do not become substantial until the 4 °C level. In that future climate, hot-hours become concentrated along the Gulf of California coast in Mexico, in the Missouri and Mississippi River Valleys, the Gulf of Mexico coast, and the Atlantic seaboard with major cities like Chicago, St. Louis, Dallas, Houston, Washington, DC, and Philadelphia having considerable accumulations of hot-hours (Table 2).

The annual accumulation of hot-hours experienced by the world's population begins to climb substantially in worlds warmer than 2 °C above the preindustrial baseline (Fig. 1F). In this study's worst-case scenario of a 4 °C warmer world, around 2.7 billion persons will experience at least 1 wk of daytime (8 h) ambient conditions associated with uncompensable heat stress, 1.5 billion will experience a month under such conditions, and 363.7 million will be faced with an entire season (3 mo) of life-altering extreme heat (Fig. 1F). There is large variability in the annual accumulations of hot-hours within regions with geography as a controlling factor (Table 2). For example, in a 4 °C warmer world, Mecca, Saudi Arabia, only experiences a mean accumulation of 142.5 h of hot-hours while 500 miles to the south, Al Hudaydah, Yemen, is projected to experience 2,407 h. When divided into equal 8-h increments, this equates to 301 d of daytime threshold exceedance per year.

Regional Heat Stress Types with Future Warming

Based on the varying T_w thresholds described in the *Introduction* and *Materials and Methods*, we investigate threshold exceedance below and above $T_a = 40\ °C$ (humid vs. nonhumid) to delineate differences in environmental impacts on physiological heat strain. Globally, across all warming levels, the substantial majority of the person-hours of threshold exceedance are characterized by humid conditions. The number of global person-hours under uncompensable heat stress conditions experienced begins to increase rapidly at +2 °C GMST, going from 86 billion person-hours at that point to 349 billion person-hours at +3 °C and 1080 billion person-hours at +4 °C with the large majority being associated with humid heat (Fig. 3A). Again, the underestimation of heat stress exposure using the previous $T_w = 35\ °C$ upper limit is readily apparent (Fig. 3A vs. Extended Data Fig. 1B) as the number of global person-hours is two orders of magnitude higher at 4 °C warming when using the updated, empirical limits.

This also reflects the large populations in South and East Asia, which, in a world that is 4 °C warmer than the preindustrial

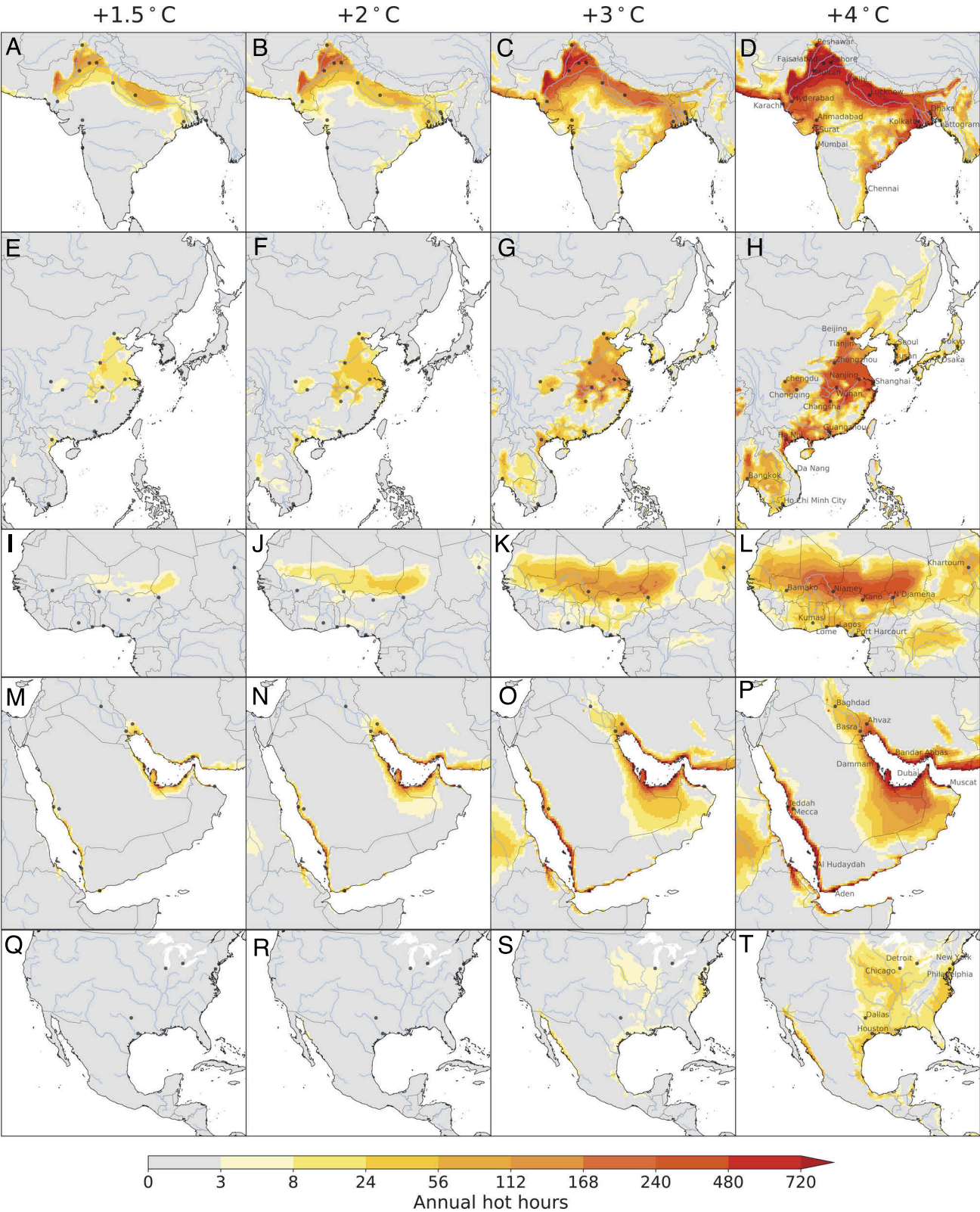**Fig. 2.** Annual hot-hours over South Asia (*A–D*), East Asia (*E–H*), North Africa (*I–L*), Middle East (*M–P*), and North America (*Q–T*) under 1.5, 2, 3, and 4 °C of warming relative to preindustrial level.

period, is projected to experience around 608 and 190 billion person-hours of threshold exceedance in humid conditions, respectively (Fig. 3 *B* and *C*). These make up 84.5% and 90.5% of their total person-hours of threshold exceedance. While the magnitude of person-hours of threshold exceedance will not be as high in sub-Saharan Africa as in Asia, even at 4 °C warming when the region will experience around 88.6 billion person-hours, the number of hot-hours associated with T_a above 40 °C is negligible (Fig. 3*D*), confirming the future impact of increasing humidity on heat stress in the region (30).

Table 2. Annual hot-hours for major cities in the world

Regions	Countries	Cities	Annual hot-hours			
			1.5 °C	2 °C	3 °C	4 °C
South Asia	India	Delhi	16.0	39.0	170.7	556.9
		Mumbai	0.0	0.2	5.9	55.4
		Kolkata	10.2	31.5	157.2	548.5
		Chennai	0.04	0.4	10.0	94.2
	Pakistan	Lahore	69.5	147.3	447.4	1,013.5
		Karachi	0.5	8.4	96.9	452.0
	Bangladesh	Dhaka	5.6	16.9	85.1	346.1
East Asia	China	Shanghai	6.9	19.1	101.4	327.6
		Beijing	4.1	13.5	54.8	127.9
		Guangzhou	1.9	6.3	49.1	274.3
		Shenzhen	0.04	0.6	9.9	115.3
	South Korea	Seoul	1.2	3.6	24.2	95.7
		Busan	1.0	3.7	25.4	93.2
	Japan	Tokyo	0.1	0.5	9.1	36.9
		Osaka	0.2	0.7	9.8	39.9
	Vietnam	Ha Noi	11.5	37.7	167.7	602.1
		Hai Phong	0.8	5.9	74.4	492.7
	Thailand	Bangkok	2.0	4.6	21.3	101.3
Middle East	Saudi Arabia	Jeddah	9.9	46.4	246.5	540.6
		Mecca	1.1	7.8	55.4	142.5
		Dammam	108.2	223.6	474.5	804.7
	United Arab Emirates	Dubai	31.9	117.7	383.9	783.9
	Yemen	Aden	57.2	203.2	815.7	1,770.2
		Al Hudaydah	98.7	340.4	1,276.3	2,407.1
	Iran	Ahvaz	7.2	18.0	64.7	173.5
		Bandar Abbas	49.9	175.5	488.7	958.6
	Iraq	Basra	4.1	10.3	39.3	117.8
Africa	Nigeria	Lagos	0.4	1.2	12.2	108.8
		Kano	0.3	1.3	47.8	175.5
	Sudan	Khartoum	1.9	5.6	42.1	103.5
	Niger	Niamey	2.0	6.4	81.5	254.9
North America	United States	New York	0.05	0.7	3.6	23.1
		Chicago	0.1	1.1	6.3	31.9

However, nonhumid conditions leading to threshold exceedance are more significant in other parts of the world. The Arabian Peninsula is projected to experience an increase in nonhumid hours of threshold exceedance in a 2 °C warmer world. By the time of a projected GMST increase of 4 °C, nonhumid person-hours of threshold exceedance are expected to be greater than 11 billion, making up more than one-quarter of all person-hours of threshold exceedance (Fig. 3E). North America, which does not experience significant exceedance of the heat stress threshold until 3 °C GMST increase, experiences the largest proportion of nonhumid days of uncompensability with 23.8% of person hours at 3 °C and 31.8% at 4 °C (Fig. 3F).

Discussion and Implications

These results indicate that a significant portion of the world's population will experience—for the first time in human history—prolonged exposures to uncompensable extreme moist heat. Humans will struggle to adapt to these conditions in a warmer world as they will present widespread challenges across many aspects of food–energy–water security, human health, and economic development including in the world's most populous and most vulnerable regions. Past research focusing on the T_w = 35 °C upper limit to human adaptability consistently highlighted the Middle East and South Asia as regions that would experience the

brunt of deadly or intolerable conditions (23), as our study does. We also find that sub-Saharan Africa may be the true hotspot of $T_w \geq 35$ °C in the future using our bias-corrected projections.

Our research shows that the footprint of life-altering heat using updated, empirically derived heat stress limits is vastly expanded. The additional regions most significantly affected are projected to be the equatorial and Sahel regions of Africa and eastern China given future warming scenarios that reach upward to 2 °C, a viable outcome by the end of the century, perhaps sooner, without drastic reductions in greenhouse gas emissions (31). Continued warming above 3 °C and 4 °C, respectively, causes North and South America, as well as northern Australia, to experience extended periods of dangerous heat. These results are another indication of the importance of restricting warming to 2 °C as suggested in the ratification of the Paris Agreement in 2015. Here, we note the differences between our study and that of a recent publication by Freychet et al. (32) and why this manuscript improves upon the former in terms of the analysis of T_w thresholds. Freychet et al. (32) found that the exposure to T_w of 31 °C (a statistically derived threshold in their study) was much more widespread than in this study, even at 1.5° and 2 °C in the Western Hemisphere and at 3 °C in parts of Europe. Overestimations in T_w are likely accrued through three main factors: 1) the use of non-bias-corrected CMIP6 data, 2) the use of daily averaged T_a and RH to calculate T_w, and 3) the use of
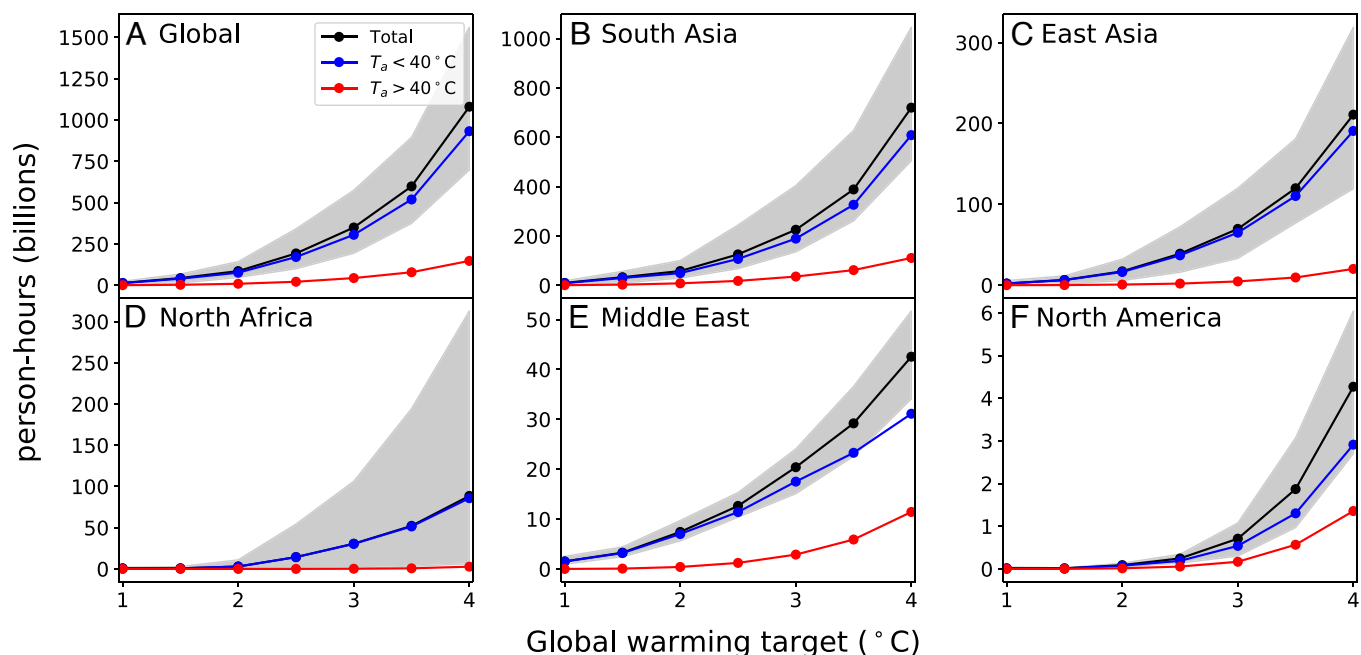
Fig. 3. (A) Global and (B-F) regional annual person-hours subject to uncompensable heat stress under 1–4 °C warming relative to preindustrial levels. Total person-hours (black) are decomposed into two parts with dry bulb temperature less (humid; blue) or greater (nonhumid; red) than 40 °C. The shaded area around black curves represents the 10th to 90th percentiles of CMIP6 model spread. The regions are defined as rectangles in Fig. 1A.

Stull's (33) equation to calculate T_w instead of Davies-Jones (34). The latter two methodological choices can each impart ~1 °C errors in the calculation of T_w (35), easily large enough to inflate values to unrealistic values given certain amounts of warming.

It is important to note that these T_w thresholds were created for a young and healthy population, albeit unacclimatized, doing minimal activity (21). This means that thresholds are certainly lower for those who are more vulnerable to the heat, either through age, body size, and morphology, comorbidities, medication use, or any physiological or behavioral impairment to thermoregulatory capacity (10). Additionally, these thresholds did not take the impact of solar radiation on human thermal balance into account which will likely also modify thresholds (36). Thus, some components of the real impact on populations are likely to be underestimated in this study. The increases in heat stress evidenced in this study must lead to changes to daily life and the need for large-scale adaptation efforts to mitigate heat stress risk.

Nevertheless, T_w above the limits found by Vecellio et al. have already been observed in regions such as South Asia, sometimes for multiple hours at a time, with lesser effects on health (37). Longer-term exposure to more intense warm season humid heat would lend itself to higher critical wet-bulb limits due to physiological, thermoregulatory adaptation (which should be confirmed with future empirical testing). Hence, in tropical and subtropical regions of the globe, where people are acclimated, our exposure metrics may overestimate vulnerability for acclimated healthy, hydrated young adults doing no work, but further study is required to establish the risk profile for other individuals and populations. The outlook in these regions is further dimmed by the fact that higher, less conservative thresholds are still breached with each degree of warming.

However, unacclimated and unacclimatized populations bear larger risks during acute extreme heat events because of their vulnerability to unfamiliar ambient conditions. Physiological acclimation to heat stress takes around 2 wk and is lost within a week after the stimulus is removed (38–40), so the infrequent heat waves which characterize mid-latitude climate dynamical regimes are unlikely to drive the kind of physiological adaptations supported by the tropical dynamical regimes. Behavioral, technological, and societal adaptation mechanisms are more likely solutions in those regions and also in higher-income tropical regions such as Singapore. This study does not directly address such adaptation and vulnerability reduction measures, but this analysis can help identify the scope and magnitude of the need for such measures.

At 4 °C warming, our worst case scenario, Al Hudaydah, Yemen, would experience threshold exceedance for 300 d a year assuming 8 h a day of the worst heat. Again, assuming even spread, every day in the year would experience at least 6 h of threshold exceedance. This would obviously be nonconducive to outdoor activities, occupational or recreational, for any extended period of time. Reliance on indoor air conditioning would become necessary to remain heat-healthy. These periods of time correlate with projected core temperatures increases associated with the clinical definition of heat stroke (25, 41). If mitigation efforts are not taken, it is likely that heat-related deaths will significantly increase due to both direct and indirect effects of the heat. However, even if indoor cooling is accessible, a quality-of-life shift would occur since a majority of a person's time will have to be spent inside for the sake of their health. Physiological adaptation is likely in particular geographic regions up to certain points given the outcomes of recent heat wave events. During an extended period of extreme heat in Pakistan in the spring of 2022, T_w values reached as high as 33 °C in Jacobabad, sometimes referred to as the "hottest place on Earth," on multiple days. Extreme dry-bulb temperatures of 50 °C also affected the Indian subcontinent during this extended heatwave. However, only 90 deaths were reported in the immediate aftermath, indicating that complex relationships between climate, health, and other socioeconomic factors must be taken in concert to develop a fuller understanding of heat-health (42).

While physiological adaptation to the heat will be one of the driving factors in the determination of the habitability of regions in the future, other adaptive measures will also need to be developed. Results showed that a large majority of the hours of uncompensable heat stress will occur at T_a less than 40 °C (50% RH or above), providing evidence that humid heatwaves will be an increasing danger in future climates (27, 43). However, as noted, climate models have a proclivity for underestimating extreme events, meaning extreme hot, dry heatwaves, perhaps exacerbated by compound local drought and subsequent land-atmosphere interactions, may be a larger factor in future heat stress than what current projections show (44, 45). Given that humid heat dominates projections and is an environmental limit to physiological adaptation, the proliferation of air conditioning, as discussed above, will be the most consequential path to ensuring livability (46, 47). This switch to widespread air conditioning will be further motivated by the fact that swamp coolers—the cooling method of choice for many lower-middle-income regions—become ineffective at high wet-bulb temperatures (48).

However, air conditioning use imparts its own contribution to exacerbating climate warming through its greenhouse gas contribution (49) and a direct sensible effluent heat flux into the local environment and an evaluation of the trade-offs will be an important future consideration. The design of future, more resilient, cities will need to take into account the type of heat it will face to maximize efficiency and utility (50, 51). While features such as green spaces, water features, and increased shade may work in regions where nonhumid threshold exceedance is more common (i.e., North America, Middle East, Australia), these factors may not be as effective or, when considering resultant added humidity from green and blue infrastructure, actually exacerbate heat stress in more humid environments (52).

Many other socioeconomic and cultural factors will also play a role in the future adaptation to heat as they have throughout history. Writing from an archaeological perspective, Rivera-Collazo (53) notes the spectrum in human responses to climate change in past civilizations, highlighting local, community-based perception to risk and subsequent adaptive capacity and mitigation efforts. They highlight specific examples such as food availability and shelter infrastructure as ways to measure social change in response to climate change. Differential vulnerability to climate change will exist (54), and gradients of adaptability (physiological, behavioral, and cultural), habitability, and survivability to extreme heat in a changing climate already do and will continue to exist on global, regional, and local scales (55) and are linked closely with socioeconomic status (56). It is important to note that a majority of the population projected to be significantly affected by the heat live in the Global South and other countries that have had the smallest effects on anthropogenic climate change but will be disproportionately harmed by its effects (57). Those who can afford to beat the heat will do so, and those who cannot will be forced to break with cultural customs to maintain a relative level of livability, but social change will be experienced by all exposed to these levels of dangerous heat stress. Hazard, risk, and vulnerability must be evaluated in tandem to understand specific health outcomes stemming from the more frequent crossing of critical environmental limits to heat stress compensability. However, it is indisputable that serious health complications on a large scale, up to and including death, will occur where environmental conditions associated with uncompensable heat stress become more frequent and longer-lasting unless behavioral or technological intervention is implemented. It is an inevitable consequence of energy balance that unless environmental conditions are changed, the positive internal heat balance must eventually lead to heat stroke. One does not need to run those physiological experiments to their unethical conclusion to understand that end result. Beyond the health impacts to the individual exposed to extraordinary heat, the magnitude to which spillover effects take place is unknown and questions as to whether these regional climate risks translate into a larger-scale climate-induced catastrophe (58). It must be the work of multidisciplinary teams of physical, health, and social scientists, especially those with specific, indigenous knowledge of those who will experience the highest risk of extreme heat due to climate change, to quantify these gradients of adaptability and survivability and provide context for just climate futures for all.

Materials and Methods

Data. T_W was calculated from 2 m temperature and specific humidity, and surface pressure at 3-h frequency from 12 CMIP6 climate models following the SSP585 scenarios (Extended Data Table 1). All variables are retrieved only from the "r1i1p1f1" member of each climate model. The 12 models were chosen because these had required output available at 3-h resolution, and the SSP585 scenario was picked to jointly maximize model ensemble size and the magnitude of the warming signal. The same variables (except 2 m dewpoint temperature in place of specific humidity) are also obtained at 3-h interval from ERA5 for calculating T_W (59, 60). ERA5 is a state-of-the-art reanalysis product, and it shows considerable improvements in tropospheric temperature, humidity, and wind compared with its predecessor ERA5-interim (61). ERA5 reanalysis serves as the "target" dataset toward which we bias-correct CMIP6 output (see the section "Bias-correction" below).

We employ global spatial population projections at a resolution of 0.125° (62, 63) to weight the estimates of annual hot-hours under different warming targets. Hot-hour estimates are interpolated to the same resolution as population data. The population projections are available for all Shared Socioeconomic Pathways (SSPs) in consistence with the national-level population and qualitative narratives within each SSP (62). Without knowing which SSP is most likely, we choose SSP2, the "middle-of-the-road" scenario. SSP2 represents a middle ground in terms of mitigation and adaptation challenges and is consistent with historical development patterns over the past century (64). The reference implementation of SSP2 amounts to an end-of-century warming of near 4 °C relative to preindustrial levels (65). Meanwhile, SSP2 also permits below 2 °C warming pending worldwide adoption of stringent climate policies (65). This flexibility to cover the range of global warming considered in this study makes SSP2 preferred. The person-hour calculation requires targeting the population projection around the time when each warming target is reached, which however comes with great uncertainties due to differing climate sensitivities of climate models. Meanwhile, global population growth in SSP2 levels off in the middle of this century, resulting in a relatively stable world population since 2040 (66). Therefore, we choose to couple SSP2 population in 2050 to all warming targets.

Wet-bulb Temperature. T_W is the temperature an air parcel would attain if water is evaporated into the air to the point of saturation with all latent heat supplied by the parcel (67). It can be measured by a thermometer covered with water-soaked cloth under a well-ventilated (3–5 m/s) condition. There are multiple ways to calculate T_W including the "isobaric" and "adiabatic" formulations (35). Here, we adopt the Davies-Jones adiabatic wet bulb temperature approach (34), which was programmed in FORTRAN (35), and incorporates temperature, humidity, and pressure data in the calculations. This formulation of T_W is substantially more accurate than more approximate forms, including the oft-used Stull approximation (27).

T_W Thresholds. Although $T_W = 35$ °C was proposed as the upper limit of human adaptability, recent empirical evidence supports lower T_W thresholds for human heat stress compensability with a multivariate dependence on T_a and RH (21).
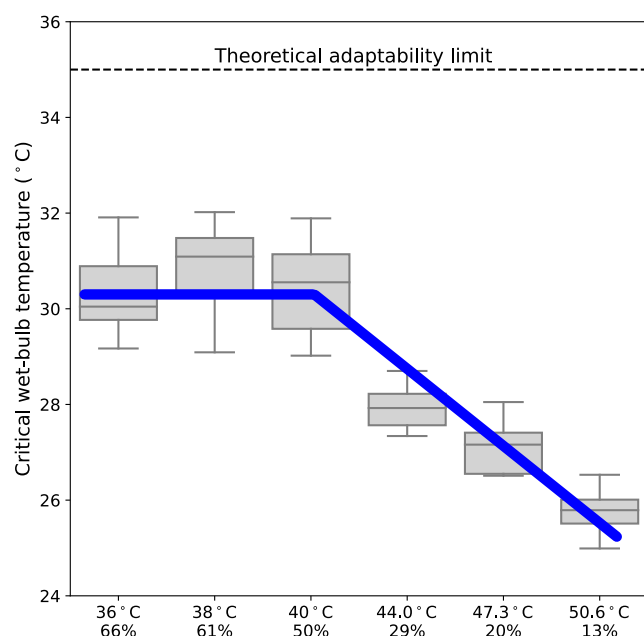
Fig. 4. T_w thresholds across a range of T_a and RH environments taken from laboratory-based measurements in young, healthy adults doing work associated with the minimal activities of daily living. Figure reprinted from Vecellio et al. (21).

Humidity variance and its role in heat stress are vital to understand in terms of how humans deal with extreme temperatures. Ambient humid heat imparts an environmental barrier on heat dissipation due to the decreased vapor pressure gradient between the skin and air. Once sweat can no longer be evaporated from the skin, which would normally lower its temperature and allow for more heat to be moved from the core to the periphery of the body to be dissipated away, the physiological mechanisms for heat stress compensability cease to exist. In hotter, but much drier environments, ambient conditions allow for free evaporation from the skin surface, but heat stress compensability is limited by a person's ability to produce sweat to be evaporated while dry heat gain rapidly increases. We attempt to account for these different types of heat by creating humidity categories based on the Vecellio et al. (21) T_w thresholds. There is no statistical difference in critical T_w values down to RH = 50% (T_a = 40 °C) (Fig. 4). Therefore, T_w thresholds in this paper consist of a constant 30.58 °C when $T_a \leq 40$ °C, which is deemed a "humid" hot-hour. From there, critical T_w decreases in a linear fashion with increasing T_a and decreasing RH given the increasing impact of dry heat gain and sweating limitations. Thus, any threshold exceedance above T_a = 40 °C is considered "nonhumid" (as moderate RHs may not be considered "dry").

Hot Exposure Projection. We apply these thresholds to future CMIP6 projections and count the annual number of hours with these thresholds being exceeded. Instead of generating results on a time-series basis following certain emission pathways, we provide estimates conditional on 1–4 °C of global warming compared with the preindustrial period in accordance with a growing interest for climate change impact assessment at discrete levels of global mean temperature increase (68, 69). The warming target-oriented approach can effectively reduce uncertainties from varying climate sensitivities of different GCMs and help generate easy-to-interpret estimates consistent with the framework of international treaties on climate change such as the Paris Agreement.

Bias-correction. Climate model output has systematic biases due to imperfect model parameterization and unresolved subgrid scale surface heterogeneity (70–73). We bias-correct CMIP6 projections with ERA5 reanalysis by superimposing CMIP6 model–simulated climate change signal onto a ERA5 baseline (1950–1976), which involves the following steps:

- We first locate the period corresponding to a warming target relative to the preindustrial era. Each year is indexed by the degree of GCM-simulated global warming. Years falling into a 0.5 °C interval centered at the warming target are selected. For example, years with 2.75 to 3.25 °C warming are chosen to represent a 3 °C warming world.
- GCM-simulated climate change signal is then derived by taking the difference of T_w and T_a at 3-h frequency between the average year of a baseline period and that of years representing a certain warming target. Note that the baseline period is chosen to be 1950–1976 (instead of preindustrial era) since ERA5 reanalysis starts at 1950 at the time of writing.
- Finally, we use bilinear interpolation to downscale GCM-simulated climate change signal to ERA5 horizontal grid spacing and add it onto ERA5 3-h T_w and T_a of each year within 1950–1976.

The bias-correction procedures above are conducted for each climate model separately spanning 1.5 to 4 °C of global warming. For every GCM under each warming target, we obtain a bias-corrected 27-y climatology sample of T_w and T_a. The 1950–1976 baseline period was chosen for two reasons. First, the relatively long time frame enables us to capture the effects of interannual natural variability. Second, global mean temperature appears to fluctuate around a relatively stable value within this period after which significant warming trends occur (74). The absence of clear warming trend during the baseline period provides us a quasi-stationary climate within the bias-corrected multiyear sample corresponding to each warming target.

GCMs output typically have coarse resolutions unable to resolve local geographic features such as lakes and coastlines where megacities tend to locate. Our bias-correction approach partially addresses this issue by adding warming signals from CMIP6 models onto ERA5 baseline climate at high resolution (0.25° × 0.25°). The warming signal, although at GCMs resolution, is expected to vary less across topography boundaries (such as coastlines) than absolute climate state does. In addition, most of the CMIP6 models do not include regional processes such as irrigation which have been shown to be important in modulating heat stress (52, 75, 76). However, these model deficiencies can only affect our results by causing biases in climate change projection which is expected to be a less significant concern than their impact on the simulation of absolute climate states.

This bias-correction approach is able to greatly improve model performance in reproducing both high and low quantiles of T_w and T_a from reanalysis products.

Author affiliations: [a]Center for Healthy Aging, Pennsylvania State University, University Park, PA 16802; [b]Earth, Atmospheric, and Planetary Sciences Department and the Institute for a Sustainable Future, Purdue University, West Lafayette, IN 47907; [c]Department of Kinesiology, Pennsylvania State University, University Park, PA 16802; and [d]Graduate Program in Physiology, Pennsylvania State University, University Park, PA 16802

1. IPCC, *Summary for Policymakers*, V. Masson-Delmotte *et al.*, Eds. (Cambridge University Press, Cambridge, UK and New York, NY, 2021), pp. 3–32.
2. S. Perkins-Kirkpatrick, S. Lewis, Increasing trends in regional heatwaves. *Nat. Commun.* **11**, 1–8 (2020).
3. S. Perkins, L. Alexander, J. Nairn, Increasing frequency, intensity and duration of observed global heatwaves and warm spells. *Geophys. Res. Lett.* **39**, L20714 (2012).
4. R. Vose, D. R. Easterling, K. Kunkel, A. LeGrande, M. Wehner, "Temperature changes in the United States" in *Climate Science Special Report: Fourth National Climate Assessment* (2017), vol. 1.
5. G. A. Meehl, C. Tebaldi, More intense, more frequent, and longer lasting heat waves in the 21st century. *Science* **305**, 994–997 (2004).
6. E. Fischer, S. Sippel, R. Knutti, Increasing probability of record-shattering climate extremes. *Nat. Clim. Change* **11**, 689–695 (2021).
7. N. S. Diffenbaugh, Verification of extreme event attribution: Using out-of-sample observations to assess changes in probabilities of unprecedented events. *Sci. Adv.* **6**, eaay2368 (2020).
8. C. Xu, T. A. Kohler, T. M. Lenton, J. C. Svenning, M. Scheffer, Future of the human climate niche. *Proc. Natl. Acad. Sci. U.S.A.* **117**, 11350–11355 (2020).
9. K. R. Weinberger, D. Harris, K. R. Spangler, A. Zanobetti, G. A. Wellenius, Estimating the number of excess deaths attributable to heat in 297 United States counties. *Environ. Epidemiol.* **4**, e096 (2020).
10. M. N. Cramer, O. Jay, Biophysical aspects of human thermoregulation during heat stress. *Auton. Neurosci.* **196**, 3–13 (2016).
11. K. L. Ebi *et al.*, Hot weather and heat extremes: Health risks. *Lancet* **398**, 698–708 (2021).
12. S. Sun *et al.*, Ambient heat and risks of emergency department visits among adults in the United States: Time stratified case crossover study. *BMJ* **375**, e065653 (2021).
13. S. A. M. Khatana, R. M. Werner, P. W. Groeneveld, Association of extreme heat and cardiovascular mortality in the United States: A county-level longitudinal analysis from 2008 to 2017. *Circulation* **146**, 249–261 (2022).
14. X. Basagaña *et al.*, Heat waves and cause-specific mortality at all ages. *Epidemiology* **22**, 765–772 (2011).
15. A. Bouchama *et al.*, Classic and exertional heatstroke. *Nat. Rev. Dis. Primers* **8**, 1–23 (2022).
16. S. C. Sherwood, M. Huber, An adaptability limit to climate change due to heat stress. *Proc. Natl. Acad. Sci. U.S.A.* **107**, 9552–9555 (2010).
17. F. Song, G. J. Zhang, V. Ramanathan, L. R. Leung, Trends in surface equivalent potential temperature: A more comprehensive metric for global warming and weather extremes. *Proc. Natl. Acad. Sci. U.S.A.* **119**, e2117832119 (2022).
18. T. Matthews *et al.*, Latent heat must be visible in climate communications. *Wiley Interdiscip. Rev. Clim. Change* **13**, e779 (2022).
19. J. S. Haldane, The influence of high air temperatures no. I. *Epidemiol. Infect.* **5**, 494–513 (1905).
20. S. C. Sherwood, How important is humidity in heat stress? *J. Geophys. Res.: Atmosp.* **123**, 11–808 (2018).
21. D. J. Vecellio, S. T. Wolf, R. M. Cottle, W. L. Kenney, Evaluating the 35°C wet-bulb temperature adaptability threshold for young, healthy subjects (PSU heat project). *J. Appl. Physiol.* **132**, 340–345 (2022).
22. C. Raymond, T. Matthews, R. M. Horton, The emergence of heat and humidity too severe for human tolerance. *Sci. Adv.* **6**, eaaw1838 (2020).
23. J. S. Pal, E. A. Eltahir, Future temperature in southwest Asia projected to exceed a threshold for human adaptability. *Nat. Clim. Change* **6**, 197–200 (2016).
24. E. S. Im, J. S. Pal, E. A. Eltahir, Deadly heat waves projected in the densely populated agricultural regions of south Asia. *Sci. Adv.* **3**, e1603322 (2017).
25. R. M. Cottle, Z. S. Lichter, D. J. Vecellio, S. T. Wolf, W. L. Kenney, Core temperature responses to compensable vs. uncompensable heat stress in young adults (PSU heat project). *J. Appl. Physiol.* **133**, 1011–1018 (2022).
26. C. Schwingshackl, J. Sillmann, A. M. Vicedo-Cabrera, M. Sandstad, K. Aunan, Heat stress indicators in CMIP6: Estimating future trends and exceedances of impact-relevant thresholds. *Earth's Future* **9**, e2020EF001885 (2021).
27. J. R. Buzan, M. Huber, Moist heat stress on a hotter earth. *Annu. Rev. Earth Planet. Sci.* **48**, 623–655 (2020).
28. Y. Zhang, I. Held, S. Fueglistaler, Projections of tropical heat stress constrained by atmospheric dynamics. *Nat. Geosci.* **14**, 133–137 (2021).
29. A. Seth *et al.*, Monsoon responses to climate changes-connecting past, present and future. *Curr. Clim. Change Rep.* **5**, 63–79 (2019).
30. A. Brouillet, S. Joussaume, Investigating the role of the relative humidity in the co-occurrence of temperature and heat stress extremes in CMIP5 projections. *Geophys. Res. Lett.* **46**, 11435–11443 (2019).
31. A. E. Raftery, A. Zimmer, D. M. Frierson, R. Startz, P. Liu, Less than 2°C warming by 2100 unlikely. *Nat. Clim. Change* **7**, 637–641 (2017).
32. N. Freychet *et al.*, Robust increase in population exposure to heat stress with increasing global warming. *Environ. Res. Lett.* **17**, 064049 (2022).
33. R. Stull, Wet-bulb temperature from relative humidity and air temperature. *J. Appl. Meteorol. Climatol.* **50**, 2267–2269 (2011).
34. R. Davies-Jones, An efficient and accurate method for computing the wet-bulb temperature along pseudoadiabats. *Mon. Weather Rev.* **136**, 2764–2785 (2008).
35. J. R. Buzan, K. Oleson, M. Huber, Implementation and comparison of a suite of heat stress metrics within the Community Land Model version 4.5. *Geosci. Mod. Dev.* **8**, 151–170 (2015).
36. Q. Kong, M. Huber, Explicit calculations of wet-bulb globe temperature compared with approximations and why it matters for labor productivity. *Earth's Future* **10**, e2021EF002334 (2022).
37. D. J. Vecellio, R. M. Cottle, S. T. Wolf, W. L. Kenney, Critical environmental limits for human thermoregulation in the context of a changing climate. *Exerc. Sport Mov.* **1**, e00008 (2023).
38. C. Williams, C. Wyndham, J. Morrison, Rate of loss of acclimatization in summer and winter. *J. Appl. Physiol.* **22**, 21–26 (1967).
39. K. Pandolf, Time course of heat acclimation and its decay. *Int. J. Sports Med.* **19**, S157–S160 (1998).
40. C. D. Ashley, J. Ferron, T. E. Bernard, Loss of heat acclimation and time to re-establish acclimation. *J. Occup. Environ. Hyg.* **12**, 302–308 (2015).
41. A. Bouchama, J. P. Knochel, Heat stroke. *New Engl. J. Med.* **346**, 1978–1988 (2002).
42. J. K. Vanos, J. W. Baldwin, O. Jay, K. L. Ebi, Simplicity lacks robustness when projecting heat-health outcomes in a changing climate. *Nat. Commun.* **11**, 1–5 (2020).
43. S. Speizer, C. Raymond, C. Ivanovich, R. M. Horton, Concentrated and intensifying humid heat extremes in the IPCC AR6 regions. *Geophys. Res. Lett.* **49**, e2021GL097261 (2022).
44. A. AghaKouchak *et al.*, Climate extremes and compound hazards in a warming world. *Annu. Rev. Earth Planet. Sci.* **48**, 519–548 (2020).
45. S. J. Sutanto, C. Vitolo, C. Di Napoli, M. D'Andrea, H. A. Van Lanen, Heatwaves, droughts, and fires: Exploring compound and cascading dry hazards at the pan-European scale. *Environ. Int.* **134**, 105276 (2020).
46. L. T. Biardeau, L. W. Davis, P. Gertler, C. Wolfram, Heat exposure and global air conditioning. *Nat. Sust.* **3**, 25–28 (2020).
47. F. Pavanello *et al.*, Air-conditioning and the adaptation cooling deficit in emerging economies. *Nat. Commun.* **12**, 6460 (2021).
48. B. Parkes, J. R. Buzan, M. Huber, Heat stress in Africa under high intensity climate change. *Int. J. Biometeorol.* **66**, 1531–1545 (2022).
49. Y. Takane, Y. Ohashi, C. S. B. Grimmond, M. Hara, Y. Kikegawa, Asian megacity heat stress under future climate scenarios: Impact of air-conditioning feedback. *Environ. Res. Commun.* **2**, 015004 (2020).
50. S. W. Myint, E. A. Wentz, A. J. Brazel, D. A. Quattrochi, The impact of distinct anthropogenic and vegetation features on urban warming. *Lands. Ecol.* **28**, 959–978 (2013).
51. M. Graça, S. Cruz, A. Monteiro, T. S. Neset, Designing urban green spaces for climate adaptation: A critical review of research outputs. *Urban Clim.* **42**, 101126 (2022).
52. V. Mishra *et al.*, Moist heat stress extremes in India enhanced by irrigation. *Nat. Geosci.* **13**, 722–728 (2020).
53. I. Rivera-Collazo, Environment, climate and people: Exploring human responses to climate change. *J. Anthropol. Archaeol.* **68**, 101460 (2022).
54. K. Thomas *et al.*, Explaining differential vulnerability to climate change: A social science review. *Wiley Interdiscip. Rev. Clim. Chang.* **10**, e565 (2019).
55. L. J. Harrington, D. Frame, A. D. King, F. E. Otto, How uneven are changes to impact-relevant climate hazards in a 1.5^{circ}C world and beyond? *Geophys. Res. Lett.* **45**, 6672–6680 (2018).
56. I. M. Otto *et al.*, Social vulnerability to climate change: A review of concepts and evidence. *Reg. Environ. Change* **17**, 1651–1662 (2017).
57. H. O. Pörtner *et al.*, "Climate change 2022: Impacts, adaptation and vulnerability" in *IPCC Sixth Assessment Report* (2022).
58. L. Kemp *et al.*, Climate endgame: Exploring catastrophic climate change scenarios. *Proc. Natl. Acad. Sci. U.S.A.* **119**, e2108146119 (2022).
59. B. Bell *et al.*, "ERA5 hourly data on single levels from 1950 to 1978 (preliminary version)" in *Copernicus Climate Change Service (C3S) Climate Data Store (CDS)* (2020).
60. H. Hersbach *et al.*, "ERA5 hourly data on single levels from 1979 to present" in *Copernicus Climate Change Service (C3S) Climate Data Store (CDS)* (2018).
61. H. Hersbach *et al.*, The ERA5 global reanalysis. *Q. J. R. Meteorol. Soc.* **146**, 1999–2049 (2020).
62. B. Jones, B. C. O'Neill, Spatially explicit global population scenarios consistent with the shared socioeconomic pathways. *Environ. Res. Lett.* **11**, 084003 (2016).
63. B. Jones, B. C. O'Neill, *Global One-Eighth Degree Population Base Year and Projection Grids Based on the Shared Socioeconomic Pathways, Revision 01* (NASA Socioeconomic Data and Applications Center (SEDAC), Palisades, New York, 2020). https://doi.org/10.7927/m30p-j498. Accessed 10 November 2022.
64. B. C. O'Neill *et al.*, The roads ahead: Narratives for shared socioeconomic pathways describing world futures in the 21st century. *Glob. Environ. Change* **42**, 169–180 (2017).
65. O. Fricko *et al.*, The marker quantification of the shared socioeconomic pathway 2: A middle-of-the-road scenario for the 21st century. *Global Environ. Change* **42**, 251–267 (2017).
66. S. Kc, W. Lutz, The human core of the shared socioeconomic pathways: Population scenarios by age, sex and level of education for all countries to 2100. *Global Environ. Change* **42**, 181–192 (2017).
67. C. Bohren, B. Albrecht, *Atmospheric Thermodynamics* (Oxford University Press, New York, NY, 1998).
68. C. F. Schleussner *et al.*, Differential climate impacts for policy-relevant limits to global warming: The case of 1.5 °C and 2 °C. *Earth Syst. Dyn.* **7**, 327–351 (2016).
69. D. Mitchell *et al.*, Half a degree additional warming, prognosis and projected impacts (HAPPI): Background and experimental design. *Geosci. Mod. Dev.* **10**, 571–583 (2017).
70. D. Maraun, Nonstationarities of regional climate model biases in European seasonal mean temperature and precipitation sums: Nonstationarities of RCM biases. *Geophys. Res. Lett.* **39**, L06706 (2012).
71. A. W. Wood, L. R. Leung, V. Sridhar, D. P. Lettenmaier, Hydrologic implications of dynamical and statistical approaches to downscaling climate model outputs. *Clim. Change* **62**, 189–216 (2004).
72. C. Chen, J. O. Haerter, S. Hagemann, C. Piani, On the contribution of statistical bias correction to the uncertainty in the projected hydrological cycle: Comparative analysis of uncertainties. *Geophys. Res. Lett.* **38**, L20403 (2011).
73. C. Piani *et al.*, Statistical bias correction of global simulated daily precipitation and temperature for the application of hydrological models. *J. Hydrol.* **395**, 199–215 (2010).
74. S. M. Papalexiou, C. R. Rajulapati, M. P. Clark, F. Lehner, Robustness of CMIP6 historical global mean temperature simulations: Trends, long term persistence, autocorrelation, and distributional shape. *Earth's Future* **8**, e2020EF001667 (2020).
75. Q. Guo, X. Zhou, Y. Satoh, T. Oki, Irrigated cropland expansion exacerbates the urban moist heat stress in northern China. *Environ. Res. Lett.* **17**, 054013 (2022).
76. S. Kang, E. A. B. Eltahir, North China Plain threatened by deadly heatwaves due to climate change and irrigation. *Nat. Commun.* **9**, 2894 (2018).
77. Eyring *et al.*, Overview of the Coupled Model Intercomparison Project Phase 6 (CMIP6) experimental design and organization. *Geosci. Model Dev.* https://esgf-node.llnl.gov/search/cmip6/. Accessed 5 August 2022.
78. D. J. Vecellio, Q. Kong, W. L. Kenney, M. Huber, Dataset for "Greatly enhanced risk to humans as a consequence of empirically determined lower moist heat stress tolerance". Zenodo. https://zenodo.org/record/8347178. Deposited 14 September 2023.